

## 8 SCIENTIFIC HIGHLIGHT OF THE MONTH: "Infrared spectrum of hydrous minerals from first-principles calculations"

---

### Infrared spectrum of hydrous minerals from first-principles calculations

Etienne Balan<sup>1,2</sup>, Michele Lazzeri<sup>2</sup>, Francesco Mauri<sup>2</sup>

<sup>1</sup> IRD- UMR 161 CEREGE, Europole Méditerranéen de l'Arbois  
BP 80, 13545 Aix en Provence cedex, France,

<sup>2</sup> Institut de Minéralogie et Physique des Milieux Condensés (IMPMC), UMR CNRS 7590,  
Universités Paris VI et VII, IPGP, 4 Place Jussieu, 75252 Paris Cedex 05, France.

Infrared spectroscopy is widely used to determine and investigate the structure of the finely divided mineral phases, which typically form in soils and weathering environments [1]. It provides information ranging from the detection and identification of specific or minor mineral constituents, hardly accessible from X-ray diffraction techniques, to the determination of the stacking order and ordering pattern of substituting cations in clay minerals [2,3]. Other applications include the mineralogical quantification in complex samples [4], the detection of mineral transformations in geological environments [5] and the investigation of the interfacial properties of minerals, through the adsorption of probe molecules [6]. Infrared spectroscopy can be performed using a large variety of experimental geometry. Concerning powder minerals, most of the spectra are recorded in the transmission mode through a rigid disk containing the powder particles diluted in a homogeneous non-absorbing matrix, such as KBr. However, other configurations can be used, such as diffuse reflectance for powdered materials [7] or attenuated total reflectance to investigate the interface between solids and aqueous solutions [6]. In complex natural samples, spectra may also be recorded from thin sections using infrared microscopy techniques [8].

The straightforward interpretation of vibrational infrared or Raman spectra is often difficult, in particular when considering finely divided and poorly ordered minerals, such as clays. On the one hand, it is experimentally difficult to measure the polarization properties of very fine particles. On the other hand, there is not always an evident relation between the microscopic atomic structure and measured vibrational bands. An additional complexity of powder spectra also arises from the influence of the shape of particles on the vibrational spectra. In fact, in polar insulators, atomic vibrations can be associated with oscillating macroscopic electric fields that are determined by the macroscopic shape of the particles. Because of all these reasons,

a theoretical determination (independent from the experiment) of the vibrational frequencies and intensities is an ideal tool to establish unambiguous relationship between the vibrational spectrum and the microscopic structure of minerals. In this context, the use of very precise first-principles computational methods based on density functional theory is extremely useful [9]. In a polar insulator, the vibrational spectrum can be obtained knowing the analytical part of the dynamical matrix and dielectric quantities such as the Born effective charges and the electronic dielectric tensor [9, 10]. These quantities can be calculated as the second-order derivatives of the total energy with respect to atomic displacements and/or an external uniform electric field, using the linear response theory [9]. Finally, the dependence of the vibrational spectroscopic properties on the dielectric properties is determined by the macroscopic shape of the considered system. Combining first-principles calculations of crystal properties with a model taking into account experimental and sample-dependent parameters, it is possible to significantly improve the comparison between theory and experiment, going a step beyond the simple comparison of the eigen values of the dynamical matrix with experimental band positions.

As a first attempt, we have investigated the infrared spectrum of kaolinite which displays well-resolved absorption bands [11]. The structure of kaolinite has been extensively investigated by neutron and X-ray powder diffraction (e.g. Ref. [12]). IR spectroscopy was also extensively used to investigate the hydroxyl groups and H-bonding pattern in kaolinite [1, 2, 13, 14]. The structure of kaolinite-group minerals is formed by a stacking of 1:1 layers (Fig. 1). Each layer contains a pseudo-hexagonal silica sheet of corner-shared  $\text{SiO}_4$  units linked to a dioctahedral sheet of edge sharing  $\text{AlO}_2(\text{OH})_4$  octahedra. Two kinds of OH groups can be distinguished. The inner-surface OH groups, which are located at the top of the dioctahedral sheet, are hydrogen-bonded with the basal plane of oxygen atoms of the next layer. Other OH groups (inner OH groups) are located inside the layer, between the dioctahedral and tetrahedral sheets, pointing horizontally toward the center of the ditrigonal cavity. Using the structure determined by Ref. [12] as an initial guess, an excellent agreement between the experimental and theoretically relaxed structure was obtained. The infrared spectrum derived from this theoretical structure is in very good agreement with its experimental counterpart (Fig. 1). A simple comparison between experiment and theory makes it possible to assign the IR bands to vibrational mode. For example, in the range of the OH stretching vibrations (Fig. 2), the band experimentally observed at  $3620\text{ cm}^{-1}$  corresponds to the inner OH stretching. The one observed at  $3695\text{ cm}^{-1}$  corresponds to the in-phase motion of the three inner-surface OH group, whereas the bands at  $3669\text{ cm}^{-1}$  and  $3652\text{ cm}^{-1}$  correspond to the out-of-phase motion of the inner-surface OH groups. This interpretation, based on coupled vibrations of neighboring OH groups, is consistent with the assignment given by Refs. [1, 14]. The previously suggested one-to-one correspondence between an IR band and a single OH group [15] is thus disproved.

The experimental position of OH stretching bands is reproduced within 1% by calculations performed using the harmonic approximation. This apparently good accuracy is however not consistent with the large anharmonicity of OH vibrations inferred from the vibrational frequency of isotopically exchanged materials [16] or from the frequency of overtones observed in the near infrared range [17]. In fact, the theoretical anharmonicity constant related to the stretching of the inner-OH group of kaolinite is  $-95.2\text{ cm}^{-1}$ , which is consistent with the experimental value of  $-86.5\text{ cm}^{-1}$  deduced from the frequency of the first overtone bands [17]. The very

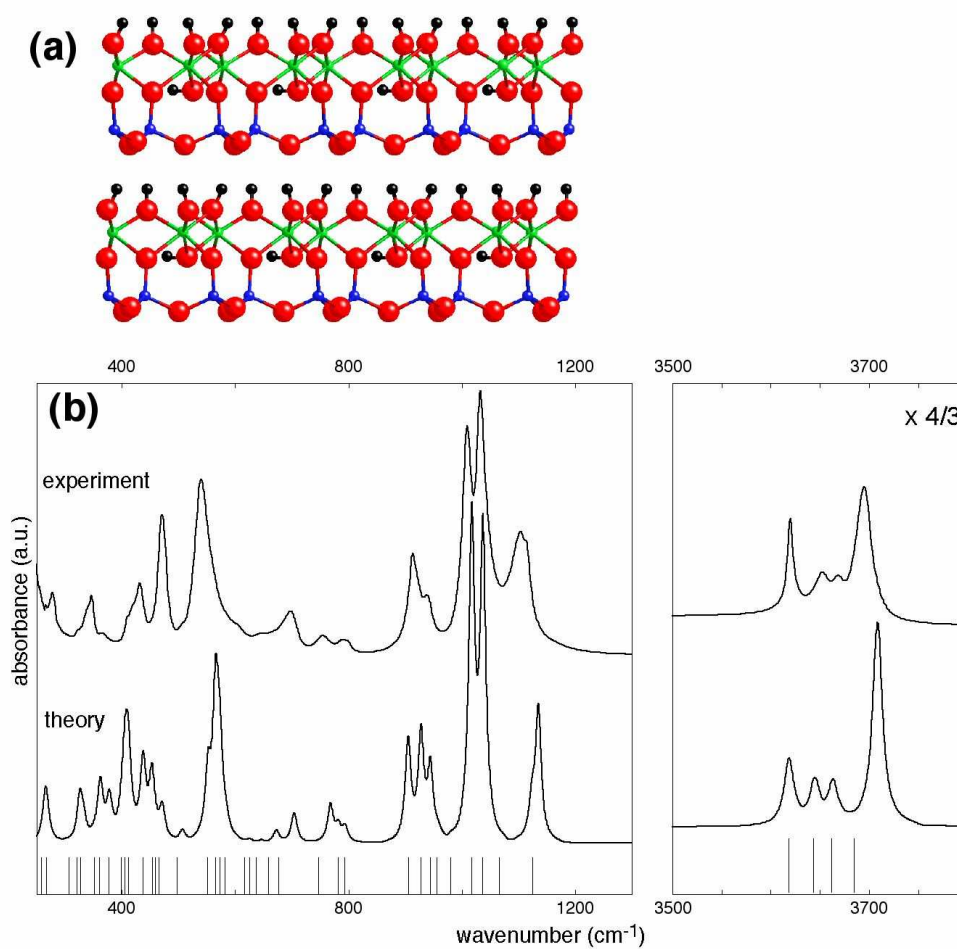


Figure 1: (a) View of the kaolinite structure showing the stacking of two layers. Note the inner-surface and inner OH groups with orientation perpendicular and parallel to the layer, respectively. (b) Theoretical and experimental infrared spectrum of kaolinite. Vertical bars correspond to the phonon frequencies. Note the very good agreement between theory and experiment making it possible to assign the absorption bands in terms of vibrational modes.

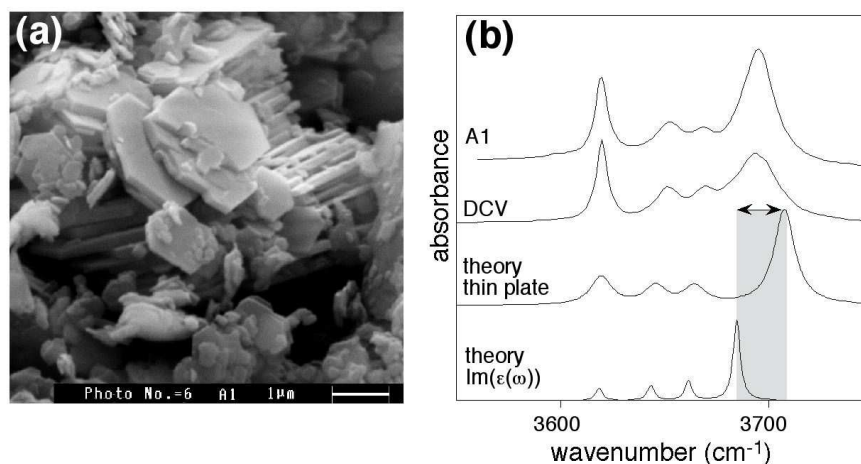


Figure 2: (a) Scanning electron micrography of a well-ordered kaolinite sample (sample A1). Note the platy shape and micrometric size of the particles. (b) Infrared spectrum of a fine (A1) and coarse (DCV) sample of kaolinite. The coarse kaolinite sample displays a significant broadening of the high frequency band. The theoretical spectrum calculated for a thin platy particle shape displays a significant shift of this band with respect to the resonances of the imaginary part of the dielectric tensor ( $\text{Im}(\epsilon(\omega))$ ), computed for a zero macroscopic electric field. For any other particle shape, the high-frequency band would occur within the shaded area; which explains the broadening observed in the coarser sample.

good agreement obtained between absolute frequencies derived from harmonic calculations and experimental frequencies thus results from the cancelation of errors related to the approximations used in DFT calculations and to the neglect of anharmonicity [18].

Further theoretical investigations have been performed on minerals displaying larger unit cell size and more complex vibrational structure. These minerals include dickite and nacrite, the polymorphs of kaolinite [19], and gibbsite, an Al hydroxide commonly found in lateritic and bauxitic formations [20]. Their structure can be described as a regular stacking of 2-layers units, each layer being related to the adjacent one by a glide plane. In the three cases, the theoretical modeling of infrared spectra enabled an unambiguous assignment of OH bands in terms of vibrational modes (see Fig. 3 for gibbsite). These investigations have shown that a significant coupling of the OH motion occurs not only between neighboring OH groups, but also between adjacent layers for the modes polarized perpendicularly to the layers. This unexpected observation underlines the long-range character of electrostatic interactions and the importance of accurate modeling tools to interpret the infrared spectra of minerals.

Effects related to long-range electrostatic interactions may occur not only in the IR spectra of structures based on 2-layers units but also in that of any fine-grained minerals, with a particle size smaller than the wavelength of the IR light (i.e.  $3 \mu\text{m}$ ). For example, the powder infrared spectrum of kaolinite reveals subtle relationships between the morphology of particles and their vibrational properties [14, 21]. Kaolinite particles indeed often display a platy shape, the basal plane of the plates being parallel to the dioctahedral layers (Fig. 2). In that case, the displacement of electrostatically charged ions perpendicularly to the layers creates a surface charge on each side of the particle, which behaves as a condensator. The surface charge induces

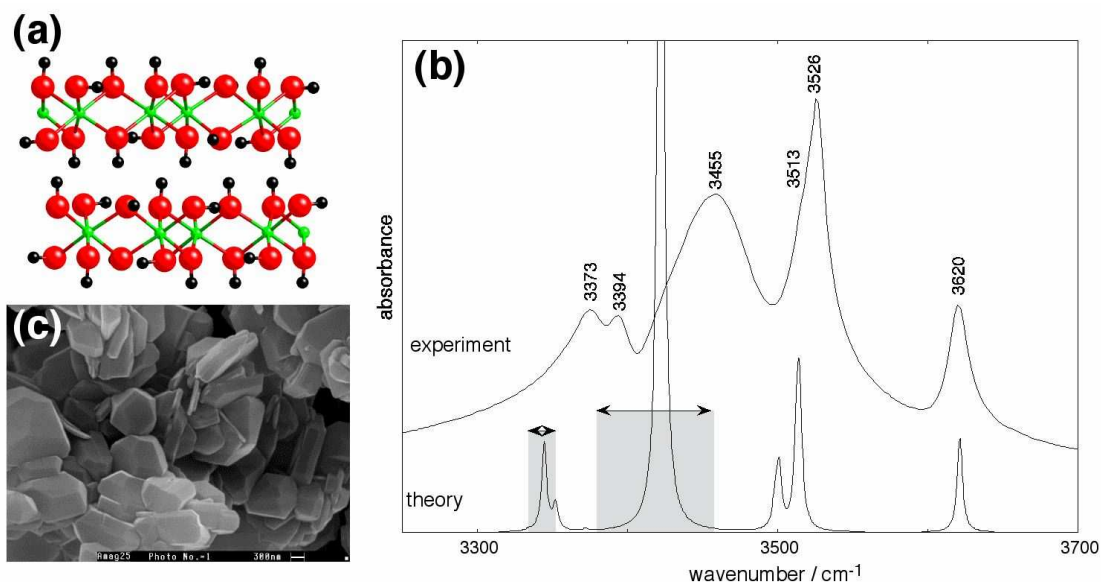


Figure 3: (a) View of the gibbsite structure ( $\alpha\text{-Al}(\text{OH})_3$ ) showing the stacking of two layers. Note that OH groups may have an orientation perpendicular or parallel to the layer. (b) Scanning electron micrography of a synthetic gibbsite sample with equant particle shape. (c) Comparison between the experimental and theoretical powder spectra of gibbsite in the range of OH stretching vibrations. The theoretical spectrum has been calculated for a spherical particle shape. Depending on the shape of gibbsite particles, intense bands polarized perpendicularly to the layers may occur within the shaded zones, explaining their significant broadening.

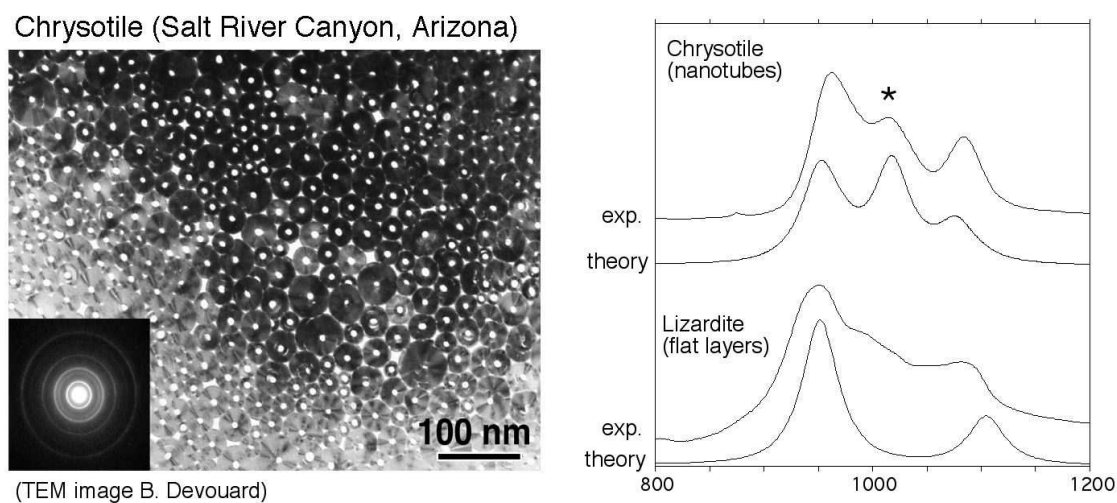


Figure 4: (a) Transmission electron micrograph of the investigated chrysotile sample (Phillips Mine, Salt River Canyon, Arizona), section perpendicular to the fiber axes. Inset: selected area electron diffraction pattern showing the parallel texture of chrysotile fibers seen along [100]. (b) Transmission powder IR absorption spectra of chrysotile and lizardite in the range of Si-O stretching bands. The theoretical spectrum of chrysotile has been computed by assuming that the chrysotile tube is a dielectric continuum, locally identical to lizardite. The comparison with experiment shows that the additional band observed in the chrysotile spectrum (star) is not related to a microscopic distortion of the structure but to collective charge excitations due to the peculiar electrostatic properties of multiwall chrysotile nanotubes.

a macroscopic electric field opposing the displacement of ions. Compared to an infinite crystal, a higher energy is thus required to displace the ions. Such increase corresponds to a higher vibrational frequency, leading to a significant blue-shift of the absorption bands. Theoretical calculations provide a quantitative modeling of this phenomenon in excellent agreement with experimental observations. For example, in the range of the stretching OH modes of kaolinite, the high frequency absorption band is related to the in-phase motion of inner-surface OH groups perpendicularly to the layers. Depending on the sample, this band may present a significant broadening, which is not related to a decreasing crystal order. Indeed, among two well-ordered samples, the broader band is observed in the most ordered one, which also displays a larger grain size (Fig. 2). In fact, theoretical calculations show that this band is shifted by  $\sim 20 \text{ cm}^{-1}$  between an infinite crystal and a thin plate of kaolinite. The thin plate geometry corresponds to the maximum shift of this band because the polarization of the corresponding vibrational mode is perpendicular to the plate. The broadening of the band therefore arises from the sensitivity of the band frequency to the particle shape, taking into account that different shapes always coexist in a given powder sample. Similar phenomena have been observed in the IR spectrum of gibbsite, which displays a strong dependence on the particle shape [22]. For a sample with relatively equant particles (Fig. 3), the best agreement between theory and experiment is obtained by considering the theoretical spectrum of spherical particles. It is noteworthy that only intense bands are significantly affected, which produces intense and broad features in the experimental spectra. The broadening is related not only to the occurrence of particles with different shape in a given sample but also to the inhomogeneity of the macroscopic electric field induced in particles whose shape differs from that of a perfect ellipsoid.

More complex effects can be observed for specific particle shapes. Particularly interesting is the case of serpentine minerals which display platy or tubular morphologies in lizardite and chrysotile, respectively (Fig. 4). Theoretical investigations have shown that the peculiar electrostatic properties of the chrysotile nanotubes leads to unexpected additional vibrational bands in the IR spectrum of chrysotile, compared with that of lizardite [23–25]. This shape-effect explains the differences recognized a long time ago between the infrared spectrum of serpentine polytypes [26] and gives a characteristic infrared signature to determine the presence of chrysotile asbestos in composite materials.

Finally, we would like to stress the importance of calculating both frequency and intensity to reach an unambiguous interpretation of the infrared spectrum of minerals. Because of the intrinsic theoretical uncertainty of mode frequency (within a few relative percents), the computation of the eigen values of the dynamical matrix only is generally not sufficient to perform a one-to-one assignment of experimental bands. In addition, the calculation of spectral intensities provides an easy way to compare theory with experiment, making the result of theoretical calculations more accessible to experimentalists.

Calculations were performed at the IDRIS institute (Institut du Développement et des Ressources en Informatique Scientifique) of CNRS (Centre National de la Recherche Scientifique) using the PW and PHONON codes (<http://www.pwscf.org>).

## References

- [1] V.C. Farmer *The infrared spectra of minerals*. Mineralogical society, London (1974).
- [2] R. Prost, A. Damene, E. Huard, J. Driard, and J.-P. Leydecker, *Clays Clay Miner.* **37**, 464 (1989).
- [3] D. Vantelon, M. Pelletier, L. Michot, O. Barres, and F. Thomas, *Clay Miner.* **36**, 369 (2001).
- [4] J. Srodon, *Miner. Mag.* **66**, 677 (2002).
- [5] Y. Lucas, F.J. Luizão, A. Chauvel, J. Rouiller, and D. Nahon, *Science* **260**, 521 (1993).
- [6] T.H. Yoon, S.B. Johnson, C.B. Musgrave, and G.E. Brown Jr., *J. Geochim. Cosmochim. Acta* **68**, 4505 (2004).
- [7] T. Delineau, T. Allard, J.-P. Muller, O. Barres, J. Yvon, and J.-M. Cases, *Clays Clay Miner.* **42**, 308 (1994).
- [8] A. Beauvais and J. Bertaux, *Clays Clay Miner.* **50**, 314 (2002) .
- [9] S. Baroni, S. de Gironcoli, A. Dal Corso, and P. Giannozzi, *Rev. Mod. Phys.* **73**, 515 (2001).
- [10] M. Born and K. Huang, *Dynamical theory of crystal lattices*, Oxford University Press, Oxford (1954).
- [11] E. Balan, A.M. Saitta, F. Mauri, and G. Calas, *Am. Mineral.* **86** 1321 (2001).
- [12] D.L. Bish, *Clays Clay Miner.* **41**, 738 (1993).
- [13] C.T. Johnston, S.F. Agnew, and D.L. Bish, *Clays Clay Miner.* **38**, 573 (1990).
- [14] V.C. Farmer, *Clay Miner.* **33**, 601 (1998).
- [15] S. Shoval, S. Yariv, K.H. Michaelian, M. Boudeulle, and G. Panczer, *Clays Clay Miner.* **50**, 56 (2002).
- [16] B. Berglund, J. Lindgren, and J. J. Tegenfeldt, *Mol. Struct.* **43**, 169 (1978).
- [17] S. Petit, A. Decarreau, F. Martin, and R. Buchet, *Phys. Chem. Miner.* **31**, 585 (2004).
- [18] E. Balan, M. Lazzeri, F. Mauri, and G. Calas, *Eur. J. Soil Science* *submitted*.
- [19] E. Balan, M. Lazzeri, A.M. Saitta, T. Allard, Y. Fuchs, and F. Mauri, *Am. Mineral.* **90**, 50 (2005).
- [20] E. Balan, M. Lazzeri, G. Morin, and F. Mauri, *Am. Mineral.* **91**, 115 (2006).
- [21] V.C. Farmer, *Spectrochimica Acta Part A* **56**, 927 (2000).
- [22] N. Phambu, B. Humbert, and A. Burneau, *Langmuir* **16**, 6200 (2000).
- [23] E. Balan, A.M. Saitta, F. Mauri, C. Lemaire, and F. Guyot, *Am. Mineral.* **87**, 1286 (2002).

- [24] E. Balan, F. Mauri, C. Lemaire, C. Brouder, F. Guyot, A.M. Saitta, and B. Devouard, Phys. Rev. Lett. **89**, 177401 (2002).
- [25] E. Balan, F. Mauri, C. Brouder, C. Lemaire, F. Guyot, A.M. Saitta, and B. Devouard, CECAM Workshop proceedings. Berichte aus Arbeitskreisen der Deutsche Gesellschaft für Kristallographie **14**, 99 (2004).
- [26] S. Yariv and L. Heller-Kallai, Clay Clay Miner. **23**, 145 (1975).